Video Article

Laser Capture Microdissection of Highly Pure Trabecular Meshwork from Mouse Eyes for Gene Expression Analysis

Caleb Sutherland*[1], Yu Wang*[2], Robert V. Brown*[1], Julie Foley[2], Beth Mahler[2], Kyathanahalli S. Janardhan[2,3], Ramesh C. Kovi[2,4], Anton M. Jetten[1]

[1]Immunity, Inflammation, and Disease Laboratory, Division of Intramural Research, National Institute of Environmental Health Sciences, NIH

[2]Cellular and Molecular Pathology Branch, Division of the National Toxicology Program, National Institute of Environmental Health Sciences, NIH

[3]Integrated Laboratory Systems Inc.

[4]Experimental Pathology Laboratories Inc.

*These authors contributed equally

Correspondence to: Anton M. Jetten at jetten@niehs.nih.gov

URL: https://www.jove.com/video/57576
DOI: doi:10.3791/57576

Keywords: Biology, Issue 136, Glaucoma, trabecular meshwork, laser capture microdissection, laser microdissection, RNA isolation, gene expression, LCM, LMD

Date Published: 6/3/2018

Citation: Sutherland, C., Wang, Y., Brown, R.V., Foley, J., Mahler, B., Janardhan, K.S., Kovi, R.C., Jetten, A.M. Laser Capture Microdissection of Highly Pure Trabecular Meshwork from Mouse Eyes for Gene Expression Analysis. *J. Vis. Exp.* (136), e57576, doi:10.3791/57576 (2018).

Abstract

Laser capture microdissection (LCM) has allowed gene expression analysis of single cells and enriched cell populations in tissue sections. LCM is a great tool for the study of the molecular mechanisms underlying cell differentiation and the development and progression of various diseases, including glaucoma. Glaucoma, which comprises a family of progressive optic neuropathies, is the most common cause of irreversible blindness worldwide. Structural changes and damage within the trabecular meshwork (TM) can result in increased intraocular pressure (IOP), which is a major risk factor for developing glaucoma. However, the precise molecular mechanisms involved are still poorly understood. The ability to perform gene expression analysis will be crucial in obtaining further insights into the function of these cells and its role in the regulation of IOP and glaucoma development. To achieve this, a reproducible method for isolating highly enriched TM from frozen sections of mouse eyes and a method for downstream gene expression analysis, such as RT-qPCR and RNA-Seq is needed. The method described herein is developed to isolate highly pure TM from mouse eyes for downstream digital PCR and microarray analysis. In addition, this technique can be easily adapted for the isolation of other highly enriched ocular cells and cell compartments that have been difficult to isolate from mouse eyes. The combination of LCM and RNA analysis can contribute to a more comprehensive understanding of the cellular events underlying glaucoma.

Video Link

The video component of this article can be found at https://www.jove.com/video/57576/

Introduction

Glaucoma is a group of diseases characterized by optic neuropathy and retinopathy that ultimately leads to irreversible blindness[1,2]. It is estimated that by 2020 over 70 million people worldwide will be living with some form of the disease[3,4,5,6,7]. Primary open angle glaucoma (POAG), the most prevalent type of glaucoma, is characterized by a decrease in aqueous humor (AH) outflow leading to increased intraocular pressure (IOP)[8,9,10,11,12,13,143,15,16,17,18]. Left untreated, chronically elevated IOP leads to progressive and irreversible damage to the retina and optic nerve head causing radial blindness[1,2,19]. All current methods for slowing the progression of glaucoma focus on reducing IOP, either by decreasing the rate of production of AH by the ciliary body or enhancing it's outflow[1,8,9,10,11,12,13,14]. The trabecular meshwork (TM) plays a vital role in actively regulating the primary AH outflow pathway and its improper function is a causative factor for hypertensive glaucoma[1,2,19]. However, the molecular mechanisms associated with TM dysfunction and how it regulates AH drainage are not yet fully understood and is currently a major focus of glaucoma research[1,2,19,20]. While several genome-wide association studies (GWAS) have linked a number of genes to glaucoma and increased resistance to AH outflow facility at the TM, the exact molecular mechanisms that lead to disease are not yet fully understood[21,22,23,24,25].

Animal models have greatly enhanced our current knowledge of disease progression in glaucoma (extensively reviewed in[3,15,16,26,27,28,29,30,31,32,33]). Several pioneering methods have been developed to study the TM[34,35,36] and these methods have been widely used to advance our current understanding of normal and diseased tissue. One area that has not been extensively explored is the use of genetically modified mouse models to study the molecular mechanisms of TM failure. Transgenic knock-in and knock-out mouse studies of TM associated genes, such as Myocilin (*Myoc*)[37,38] and *Cyp1b1*[39], have been the primary tools for studying the molecular mechanisms of TM function. Understandably, the small size of the TM in mice represents a serious hurdle that must be overcome in order to begin to study this tissue. Mouse models represent a powerful tool for studying the genetics and molecular mechanisms of disease, while advances in LCM technologies provide the necessary tools to empower the study of the smallest and most delicate tissues, including the TM.

In this report, a robust and reproducible method is described for the LCM of highly enriched TM from mouse eyes along with subsequent RNA isolation, and amplification for downstream expression analysis. Similar methods have been used successfully in mice to isolate other types of eye tissues[40,41,42,43,44], the methodology reported herein can be applied to other discrete tissues of the eye to study RNA, microRNA, DNA, and proteins. Importantly, this technique enables the use of genetically modified mice to better understand the molecular pathogenesis of TM impairment in glaucoma and ocular disease[3,15,16,17,18,26,31,45,46]. The ability to isolate the TM of mouse eyes by LCM will be a useful technique in obtaining further insights into the molecular mechanisms of several ocular diseases.

Protocol

The National Institute of Environmental Health Sciences (NIEHS) Animal Care and Usage Committee (ACUC) approved all methodology of this study under the NIEHS Animal Study Proposal IIDL 05-46.

1. Optimal Tissue Collection for Laser Microdissection

1. Obtain 2 to 3-month-old mice, male or female C57BL/6. Euthanize with CO_2 for a minimum of 1 min or until respiration has ceased. Remove the animal from the cage and assure death by either cervical dislocation, decapitation, or thoracotomy.
2. Before dissection, ensure all dissection tools are clean and sterilized.
   NOTE: For the removal of the eyes curved scissors and forceps with serrated tip (preferred tip size: 0.5 x 0.4 mm) will be needed.
3. Lay the mouse down on a flat surface on its side so that the eye is easily accessible. Grasp onto the canthus (corner of the eye) with the forceps to stabilize the mouse, then using the curved scissors, facing the curve away from the eye, cut around the eye using the eye socket as a guide until eyeball can easily be taken from the socket (use the curve not the tips of the scissors).
4. Gently pull and, using the curved scissors, cut the optic nerve, which releases the eye from the orbital socket. Carefully remove non-ocular tissue from the eye and rinse in 1x phosphate buffered saline (PBS). Repeat 1.3 - 1.4 for the contralateral eye.
5. Blot the eye with a tissue wipe to remove any moisture before embedding. Place the eye into specimen mold (25 x 20 x 5 mm^3) so that the lens and optic nerve are parallel to the bench top in order to obtain sagittal sections. Embed eyes in Optimal Cutting Temperature (O.C.T.) compound and place on the dry ice to freeze. Once frozen, store the blocks at -80 °C.

2. Frozen Section Preparation for Laser Microdissection

1. Before use incubate polyethylene terephthalate (PET) membrane slides in UV cross-linker at maximum power for 45 min.
2. Spray RNase decontamination solution onto the brush, forceps, coupling jars, and mounting chuck. Wipe thoroughly. Rinse with nuclease-free water and dry. Wipe down the cryostat with 100% ethanol to avoid cross-contamination.
3. Adjust cryostat to -18 °C. Remove one frozen block from -80 °C freezer at a time and deliver to the cryostat with dry ice. Allow frozen block to equilibrate with the temperature of the cryostat for a minimum of 10 min.
4. Squeeze a small amount of O.C.T. onto the mounting chunk (**Figure 1A**) and remove the tissue block from the mold and carefully place the block on the mounting chuck (**Figure 1B**). Once the tissue block on the mounting chuck is frozen solid, insert onto the specimen holder of the cryostat (**Figure 2A**).
5. Adjust the cryostat to cut 8 µm sections and carefully section through the O.C.T. block to reach the tissue sample. Once the tissue is observed, stop sectioning, trim the frozen blocks on all sides using a clean razor blade and leave 3 - 4 mm of O.C.T. surrounding the tissue to enable handling with the paint brush (**Figure 2B**). Use a new clean paint brush instead of the roll plate between each sample change to avoid the sample cross-contamination.
6. Section through the eye working quickly. Stain every third section by flooding the slide with a quick one-step hematoxylin and eosin (H&E) stain for 60 s, rinse with tap water, air dry, clear in clearing agent and mount on a charged glass slide with a coverslip. View under the microscope and continue sectioning until the TM is evident in the cut sections.
7. Once the TM starts to appear, cut 2 sections and mount onto a charged glass slide for routine H&E staining to form a map for cutting with LCM.
   NOTE: See Section 3 for map and staining details.
8. After the first H&E map slide, cut and line up 6 serial 8-µm thick sections in the cryostat and simultaneously mount onto the PET membrane slide (**Figure 3A, B**). Adhere the tissue by briefly sliding gloved thumb along the back of the membrane. After mounting, place the PET membrane slide immediately into a slide box on dry ice.
   NOTE: Fewer sections may be mounted, however, mounting multiple sections onto the slide at once is recommended to reduce RNA degradation by limiting the amount of time each section is exposed to the room temperature air.
9. Continue to section the eye, after every two PET membrane slides with 6 sections each, collect two sections on a charged glass slide to create another map slide for H&E staining. Continue sectioning, approximately 100 serial 8-µm thick sections, until TM is no longer visible. Confirm by quickly staining one section on a charged glass slide (See 2.6).
10. Store all PET membrane slides at -80 °C for later LCM use.

3. H&E Map Slide Staining Protocol and Morphological Review

1. To visualize and review the map slides on the charged glass slides, fix the tissue by transferring immediately into a staining jar filled with 100 mL of the rapid fixing solution for 7 s. Rinse the slide by dipping it into distilled water 10 - 20 times, then transfer the slide to a coupling jar with clean distilled water.
2. Remove the slide from water and blot dry edges with tissue wipe. Pipette 200 µL modified filtered Harris Hematoxylin onto each section and incubate for 30 s at room temperature. Carefully rinse the slide under running tap water until water runs clear. Blot the end of the slide with a tissue wipe between each step (blot between each step from 3.2 - 3.5) to remove excess liquid.
3. Place slide in 1x PBS at room temperature for 30 s. Then, carefully rinse the slide under running tap water for 30 s.

4. Dip the slide 3 - 4 times into 95% ethanol bath. Apply enough Eosin Y dye solution to cover the tissue on the slide and incubate for 15 s at room temperature.
5. Rinse the slide in 95% ethanol bath two times with 10 - 20 quick dips each. Rinse the slide in 100% ethanol bath two times with 10 - 20 quick dips each. Then, rinse slide two times in xylene bath (10 - 20 quick dips each).
6. Mount by applying resinous mounting medium to the tissue, add coverslip carefully to avoid air bubbles and let it dry in the hood overnight.
7. Review H&E slides visually or by using a digital slide scanner. Identify map slides with TM clearly visible and accessible for cutting. Use the PET membrane slides between these map slides for LCM.

4. Polyethylene Terephthalate (PET) Membrane Slides Processing and Staining Protocol

1. Before removing PET slides from freezer first prepare cresyl violet stock solution by dissolving 0.3 g cresyl violet acetate in 20 mL of 75% ethanol and place onto shaker for 2 h. Filter the solution with 0.22 µm sterile filter unit and store at 4 °C for no longer than 6 months.
2. Prepare eosin Y alcoholic solution with fresh 75% ethanol at a 1:4 ratio. Prepare fixation (75% ethanol) and dehydration solutions (75%, 95%, & 100% ethanol) in the clean, nuclease-free, 50 mL conical polypropylene tubes on ice. Add RNase Inhibitor to each solution.
3. Remove the slide box containing frozen tissue sections from -80 °C freezer and place it on dry ice. Process one slide at time. Fix slides by placing the slide immediately into cold 75% ethanol for 30 s.
4. Gently dip the slide in nuclease-free water for 10 - 15 s to dissolve O.C.T. without interfering with the tissue sections.
5. Carefully pipette 300 µL of 1.5% cresyl violet acetate solution directly onto the sections and incubate for 45 s at room temperature. Then, wash one time by placing it into 75% ethanol bath for 30 s. Pipette 200 µL eosin Y solution onto the sections and incubate for 3 - 5 s.
6. Dehydrate tissue by placing the slide subsequently in 75% ethanol, 95% ethanol, and finally, 100% ethanol bath for 30 s each. Blot the end of the slide with a tissue wipe between every step to remove excess liquid. Let the slide air dry completely under the hood for 5 min. Once dry, perform LCM immediately thereafter.
   NOTE: It is recommended to avoid the use of xylene for this step, it can cause tissue sections to inadequately bond to the membrane slide and reduces the efficiency of tissue capture.

5. Laser Microdissection with UV Laser

1. Turn on the computer and allow to boot. Turn on the microscope white light power supply. Turn on the UV laser key and a yellow LED will illuminate. Start the LCM software, allow it to load fully and a live video will display. Press the laser button on the controller box and a green LED will illuminate.
2. Load a new glass slide onto the microscope stage, then place the PET membrane slide with the stained tissue side facing down directly on the top of the glass slide. Make sure the membrane and the glass slide are paired tightly on the microscope stage.
3. Start LCM by first setting the slide limits. Choose the lowest 4X magnification in the objective panel (**Figure 4**). Then define the work area of the membrane slide by moving the microscopes xy-stage until the upper left corner where the metal and membrane meet is visible in the live video feed, press the "Limit 1" button and a red rectangle will appear on the roadmap. Next, move to the xy-stage to the opposite corner and press the "limit 2" button. Press the "scan" button to create a roadmap image of the membrane and tissues between the set limits.
4. Double click near the TM of one of the eye sections within the roadmap, the TM can be located near the apex of the iridocorneal angle (**Figure 5A**). Once the TM has been identified, increase the magnification to 10X and manually focus on the TM. Repeat with 20X and 40X objectives. When the TM is in focus with the 40X objective (**Figure 5B**), navigate into a blank area nearby (focus may need to be slightly adjusted), select the "freehand drawing tool" and draw a long line on a blank area of tissue.
5. Set the laser parameters so that the "cut velocity" is 34%, "focus" is 58%, and "power" is 70% (**Figure 4**), then press the "cut" button. Make fine laser adjustments to the speed, focus, and power parameters until a clear and fine cutting line is observed (See **Figure 5C**). For precise cutting, ensure cutting action follows the drawn line.
6. Load the isolation tube lid into the cap holder and open the tube. Attach the cap-holder to the cap-lift and make sure the tube is inverted. Assure that the adhesive cap material protrudes beyond the tip of the cap to ensure that the desired tissue is properly captured.
7. Select the "Manual" dissection mode in the software panel. Carefully review that the TM (**Figure 5B**) is directly beneath the isolation tube. Set the white balance and adjust brightness to acquire optimal image quality (**Figure 4**).
8. To begin cutting, manually adjust the focus and draw a line using the freehand tool, be sure that the collection cap remains in the up position not yet touching the membrane. Draw partial circles near where the TM meets the sclera (**Figure 5C**), then press "cut." Once the first cuts are done, position the cap into the down position and re-adjust the focus, then draw two lines in the open or free space to connect the two partial circles completing the circle around the TM, then press "cut" and collect tissue from section, ensure that the TM was picked up by the microdissection cap (**Figure 5D-F**).
9. Position the cap back into the up position and repeat (5.2 - 5.8) on the remaining sections. Slightly adjust the cap position so all the isolated samples will fit onto the cap and not overlap (**Figure 5G**). For consistency, the time window for one slide is 20 min. Use fewer sections per PET slide if more time is needed for isolating TM from all sections. For the next PET membrane, insert a new isolation tube and repeat section 5.

6. Lysis of Microdissected TM Tissue

1. Freshly prepare RNA lysis buffer to lyse LCM isolated tissue. Add 10 µL β-mercaptoethanol to each 1 mL of the lysis buffer. Store the lysis buffer with β-mercaptoethanol at room temperature for no longer than 1 month.
2. Remove the isolation tube from cap holder within 20 min from the start of the microdissection. Visualize the cap surface by eye to ensure the capture of TM.
3. Carefully pipette 10 µL lysis buffer onto the lid of the collection tube ensuring the lysis buffer completely covers the microdissected TM. Gently close adhesive cap and incubate collection tube upside-down at room temperature for 10 min. After incubation, centrifuge at 800 x g for 2 min and place lysate on dry ice. Store lysates at -80 °C for later purification and analysis.

7. RNA Isolation and Analysis of Quality

1. Analyze the RNA quality by thawing samples at room temperature. Pool together all samples isolated from a single mouse into one RNase-free 1.5 mL microfuge tube.
   NOTE: For example, for each biological replicate, 10 - 12 tubes with microdissected caps in 10 µL lysate were generated and all lysates were transferred into a single tube for each biological replicate (100 - 120 µL lysate).
2. Add one volume of freshly prepared 70% ethanol (made with RNase-free water) to each lysate solution. Then, purify total RNA following the RNA isolation kit user guidelines. Ensure the removal of genomic DNA from each RNA sample.
   NOTE: Genomic DNA can interfere with downstream RNA analysis.
3. Measure the quality of RNA isolated from the TM by pooling together samples from each mouse and analyzing the ribosomal RNA integrity (**Figure 6A**).
   NOTE: Due to the small size of the TM, ribosomal RNA peaks may not be observable (**Figure 6B**) on the RNA quality profile (two peaks observed between 1,000 - 4,000 bp in **Figure 6A, C**) which is used to calculate the RNA integrity number (RIN)[47].
   1. Obtain a more accurate measure of RNA integrity by isolating RNA from the more abundant remaining tissue on the membrane slide. To obtain a representative RIN, isolate RNA from the ocular-tissue on the membrane slide by pipetting 10 µL lysis buffer onto one tissue section and perform RNA isolation. Analyze RNA quality and calculate RIN (**Figure 6C**).
4. For downstream RNA applications, use a low input RNA kit for sequencing and cDNA library generation to yield reproducible results from as little as 80 sections of LCM isolated TM.

8. Analysis

1. To verify that the tissue collected is in fact enriched in TM-associated genes, collect multiple additional RNA from microdissected whole eye, sclera, iris, retina, cornea, and lens from 3 separate mice. Use this RNA in combination with LCM collected RNA from isolated TM and ciliary body collected from 4 separate mice.
2. Convert the RNA from the microdissected samples was to cDNA using a cDNA reverse transcription kit. Amplify the RNA from LCM isolated samples and convert to cDNA using a low input RNA to cDNA kit.
3. Analyze all RNA for trabecular meshwork expressing genes, myocilin (*MYOC*) and alpha-actin-2 (*ACTA2*), and normalize using the *HSP90a1* housekeeping gene by digital PCR (**Figure 7A-B**).

Representative Results

LCM collected RNA from the TM and ciliary body from 4 different mice was isolated in order to be able to analyze gene expression and compare the expression with that in whole eye, sclera, iris, retina, cornea, and lens isolated from three separate mice. TM expressing genes, *MYOC*[48] and *ACTA2*[49] were analyzed in all the collected tissues to confirm that the isolated TM samples were indeed highly enriched in TM. Due to the extremely low quantity of cDNA from the LCM samples digital PCR was used, which has been proven to be more reproducible with less material[50]. The expression of *MYOC* and *ACTA2* was normalized using the *HSP90a1* housekeeping gene, then each tissue was compared to that of the whole eye. These results show that *MYOC* (**Figure 7A**) and *ACTA2* (**Figure 7B**) are highly expressed in the TM samples, confirming the successful isolation of high quality RNA from the highly enriched TM samples for downstream RNA analysis. As proof of concept, this technique was applied to the TM-isolated RNA prepared from WT mice and from a strain of mice with an elevated IOP phenotype and analyzed by microarray. This analysis identified many genes implicated in glaucoma that are differentially expressed between the TM of WT mice and those of the mice with the glaucoma phenotype (**Figure 7C**).

A

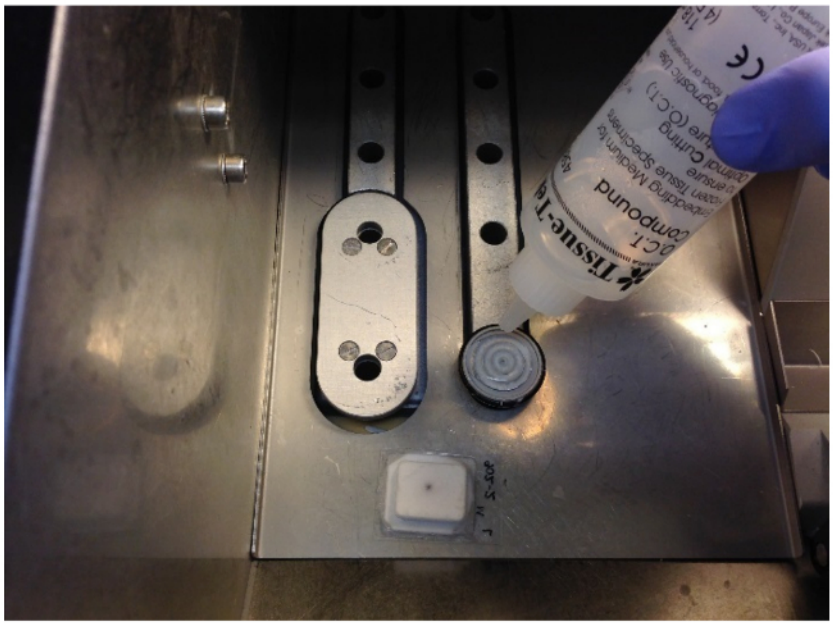

B

Figure 1: Placement of frozen tissue block in the cryostat. (A) O.C.T mounting medium is applied to the cryostat mounting chunk. **(B)** Frozen specimen block is evenly placed on the mounting chuck. Please click here to view a larger version of this figure.

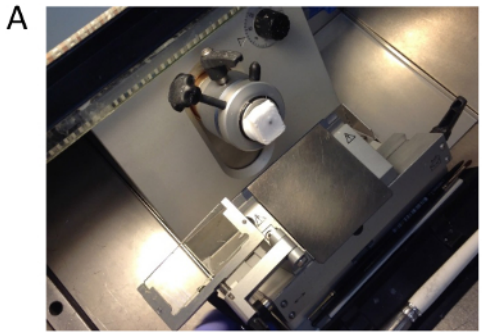

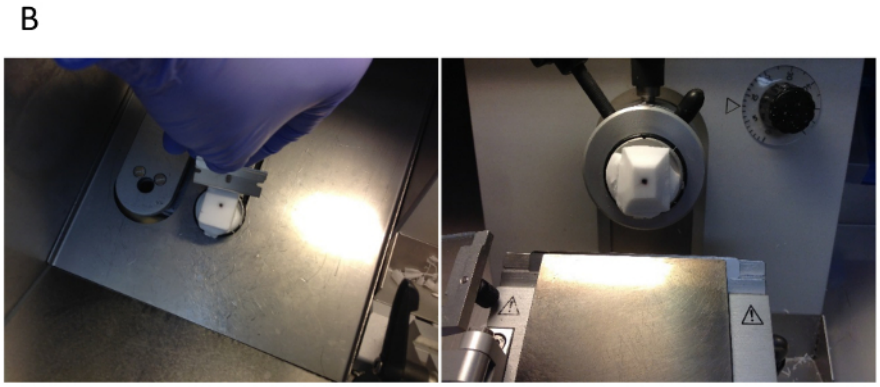

Figure 2: Sectioning procedure of frozen eye tissue in the cryostat. (A) Preparation of cutting surface to reach eye tissue. **(B)** Trimming O.C.T. of the frozen block before collecting sections for laser microdissection. Please click here to view a larger version of this figure.

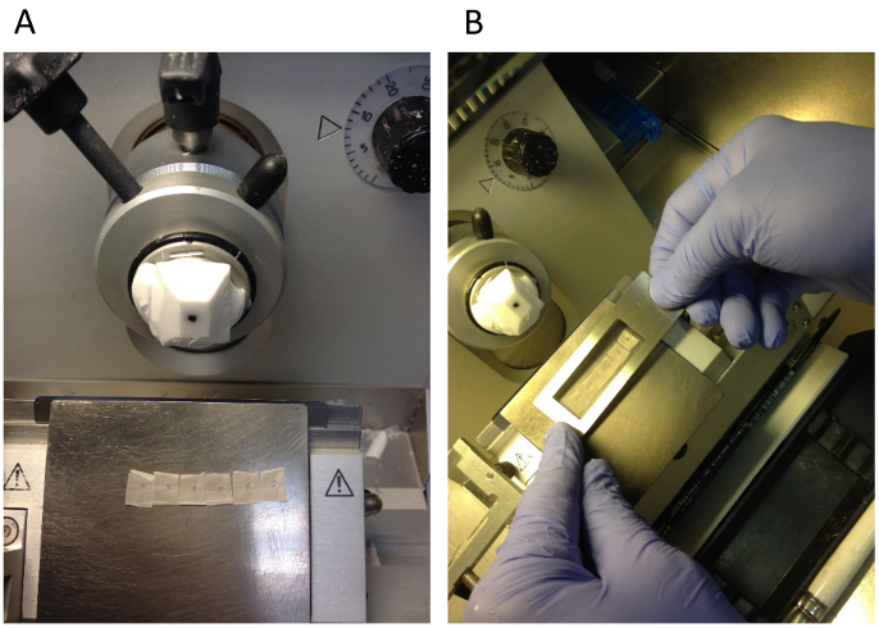

Figure 3: Preparation of frozen sections in the cryostat. (A) 6 serial 8 µm thick sections are lined up in the cryostat. **(B)** Sections are simultaneously mounted on the PET membrane slide. Please click here to view a larger version of this figure.

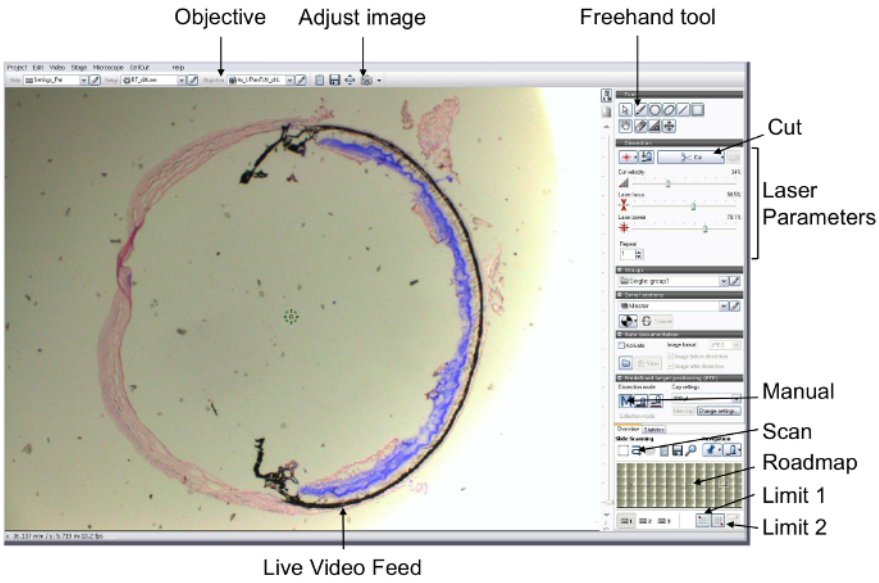

Figure 4: Screenshot of laser microdissection software highlighting important features. Please click here to view a larger version of this figure.

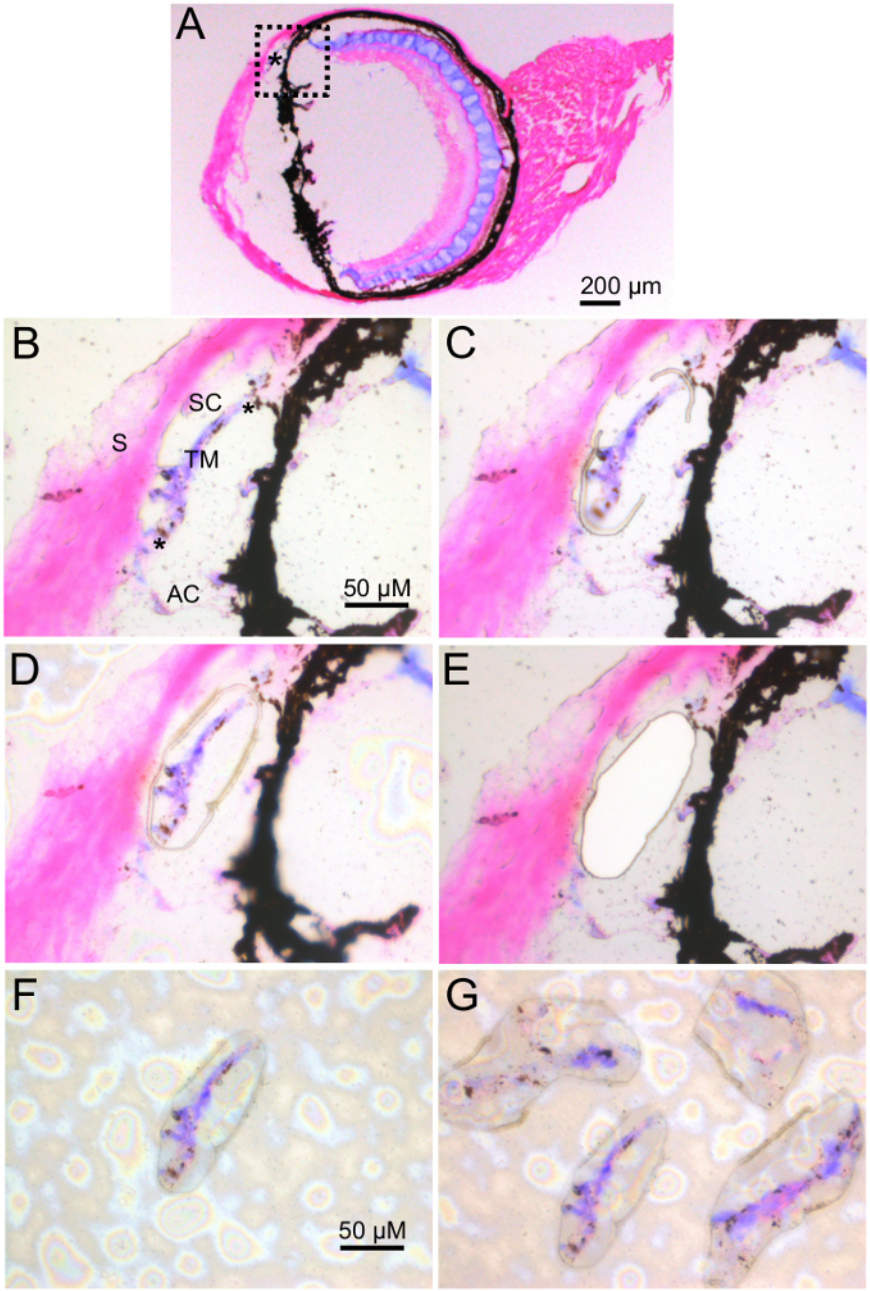

Figure 5: Location of trabecular meshwork and UV laser parameter settings for proper isolation of trabecular meshwork. (A) Low (4X) magnification of a single section on the PET membrane highlighting the trabecular meshwork for laser microdissection. **(B)** High (40X) magnification of trabecular meshwork and adjacent tissues. **(C)** First partial circle cuts of the TM near the scleral region with the cap in the up position. **(D)** Final cuts in the free space that complete the circle around the TM with the cap in the down position. **(E)** TM removed from the section and **(F)** attached to the cap. **(G)** Multiple cut sections cut from the same PET membrane not overlapping adhered to the cap. **S** (Sclera), **SC** (Schlemm's Canal), **TM** (Trabecular Meshwork), **AC** (Anterior Chamber). Please click here to view a larger version of this figure.

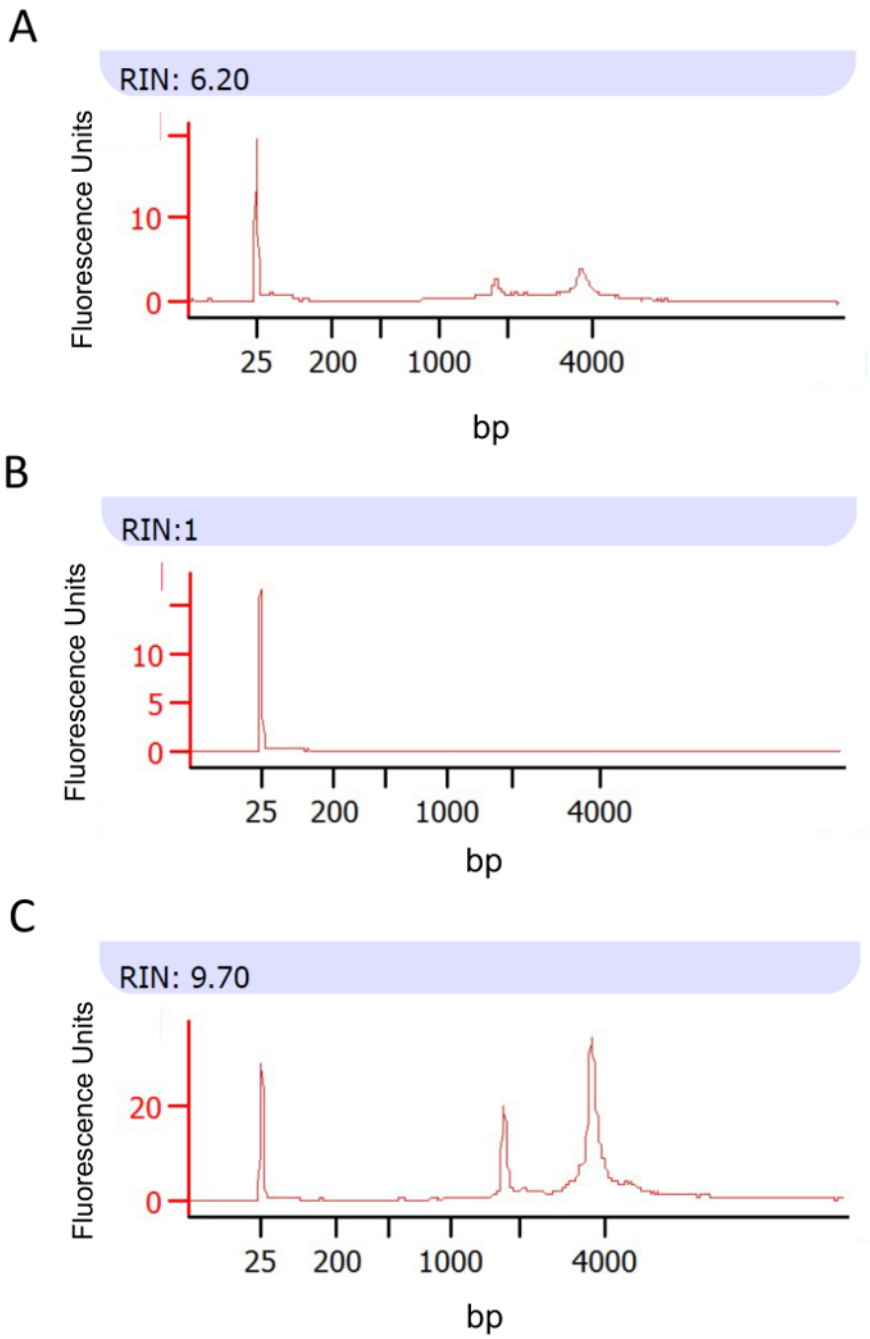

Figure 6: Total RNA yield and quality estimation obtained from microdissected trabecular meshwork tissue. (A) Total RNA from 80 sections of trabecular meshwork (approximated area size was 0.8mm^2). **(B)** Total RNA from 20 sections of trabecular meshwork (approximated area size was 0.2mm^2). **(C)** Total RNA from remaining eye tissue after laser microdissection. RIN, RNA integrity number; bp, base pairs. Please click here to view a larger version of this figure.

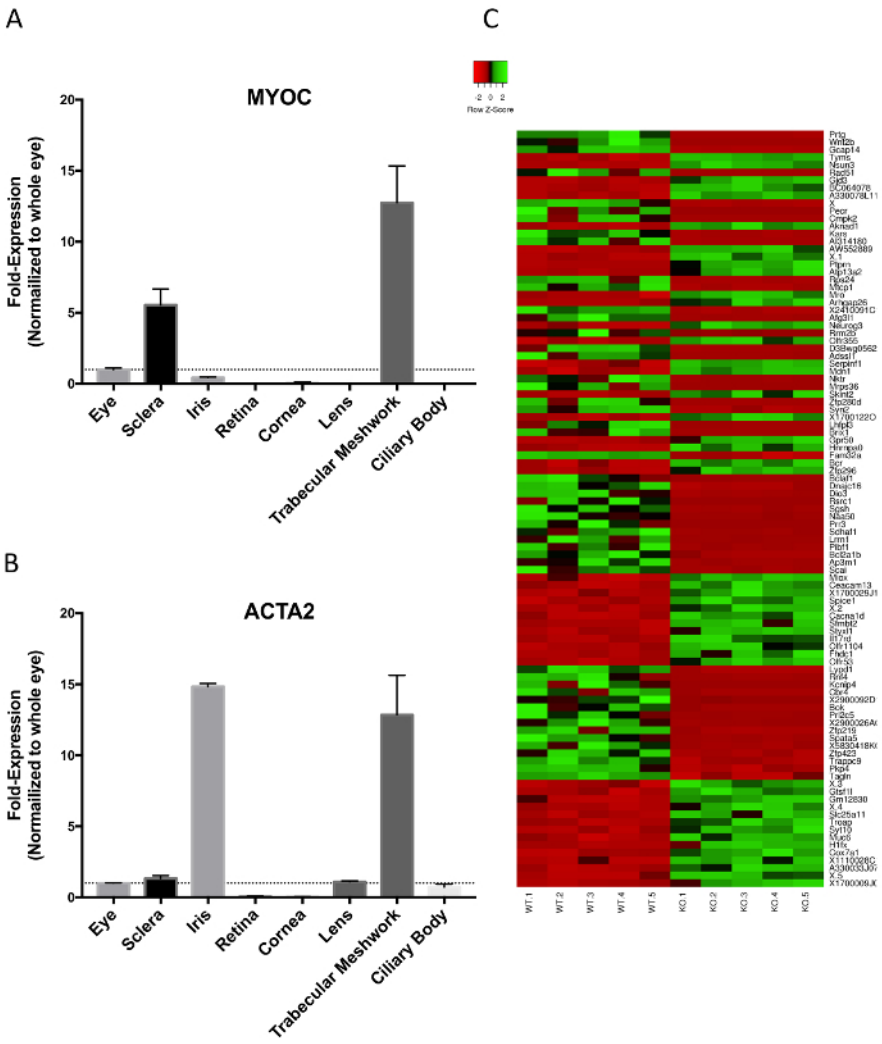

Figure 7: Downstream RNA analysis of LCM isolated trabecular meshwork. Quantitative digital PCR analysis of TM-associated genes in the TM isolated by LCM. The TM-associated genes **(A)** *MYOC* **(B)** *ACTA2* highly expressed in the LCM captured TM samples compared to other eye tissues. **(C)** Heatmap generated from data obtained from microarray analysis of trabecular meshwork RNA isolated from WT mice and KO mice with an elevated IOP phenotype. Please click here to view a larger version of this figure.

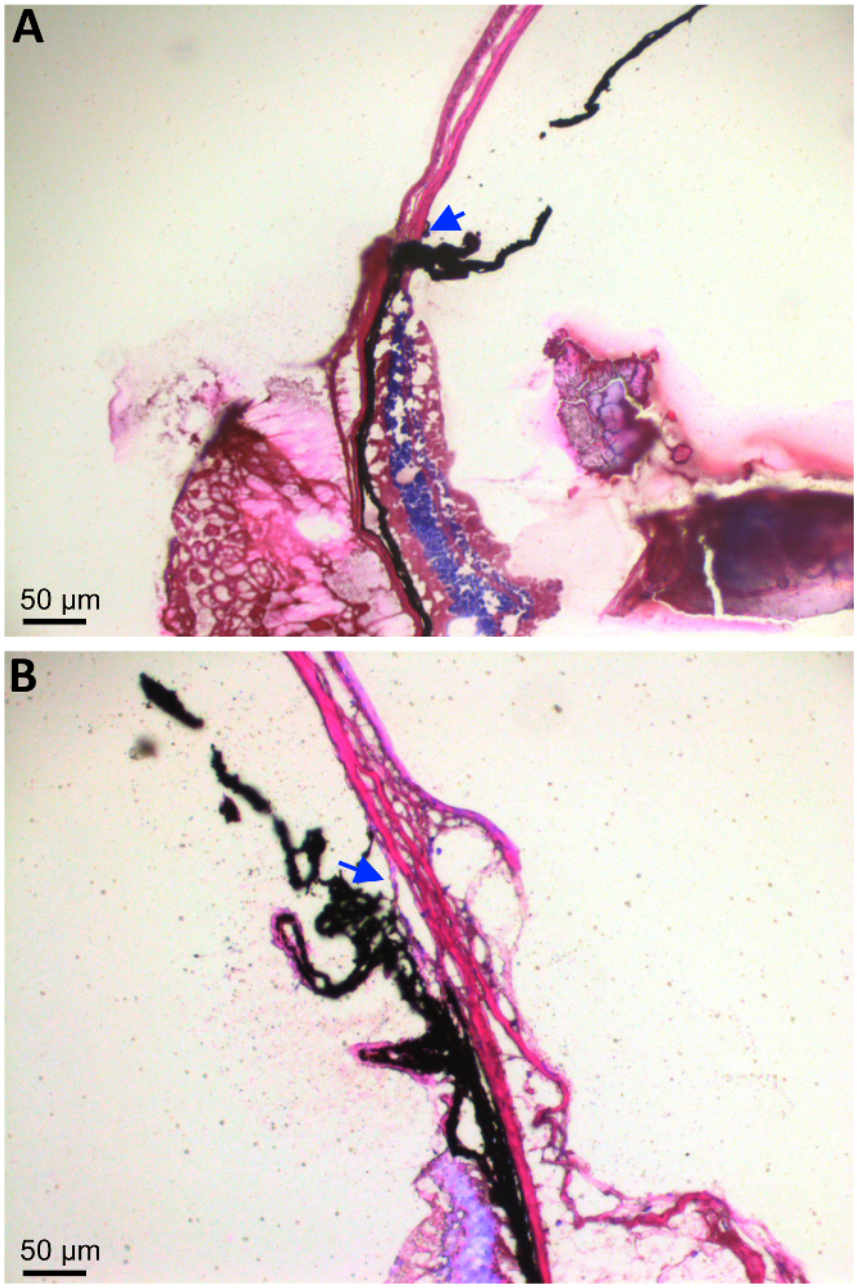

Figure 8: Comparison of tissue preparation before and after optimization. Eye sections cut and placed on PET membrane slides either with **(A)** the standard 95% ethanol dehydration preparation **(B)** or the optimized 75% ethanol dehydration preparation. Please click here to view a larger version of this figure.

Discussion

The TM plays a vital role in actively maintaining homeostatic IOP and its dysfunction is widely accepted as the main causative factor for hypertensive glaucoma[1,2,19]. A number of single nucleotide polymorphisms in several genes identified by GWAS analysis have been linked to increased glaucoma risk and increased resistance to AH outflow facility at the TM; however, the precise molecular mechanisms that give rise to this disease are not yet fully understood[21,22,23,24,25]. Genetic mouse models can provide a powerful tool for studying the molecular mechanisms of glaucoma. However, the small size of mouse TM tissue represents a formidable challenge for isolation of highly-enriched TM from mouse eyes and high quality RNA for gene expression analysis. LCM is a valuable technique for isolating a single or low number of cells and can be used to study gene expression in tissue samples enriched for specific cell types. In this study, a robust and reproducible LCM method is described to isolate highly enriched TM and high quality RNA that can be used to study the regulation of gene expression and cell signaling in the TM. In addition, the described LCM method can also be applied to other tissues within the eye.

LCM technology and a high attention to detail for optimization of tissue handling played a vital role in the successful development of this method. The methodology of tissue preservation and isolation is a key component in isolating high quality RNA for gene expression profiling. LCM requires a very high attention to detail in dissecting, cryosectioning, fixation, staining, dehydration, and time duration of laser microdissection to be successful in obtaining quality RNA[51]. Tissue section thickness can be increased; however, as the thickness increases so does the UV laser power needed. Increased laser power results in a wider laser path that can cause RNA degradation. It was found that the laser path with 8 µm sections was thin and provided enough tissue for downstream RNA analysis. **Figure 8** shows how optimization of the tissue preparation can drastically alter the ability to laser dissect the TM from the eye. The optimization of this step in the protocol (as described in section 4) yielded superior ocular-tissue immobilization and complete removal of O.C.T. (**Figure 8B**) by simply using 75% instead of 95% ethanol (**Figure 8A**) to dehydrate the tissue followed by incubation in RNase-free water to remove mounting media. Further dehydration and staining is achieved by using alcohol-based staining reagents. In addition, it was found that alcohol-based staining reagents yielded superior results relative to aqueous staining reagents (water-based cresyl violet or hematoxylin) and further helps preserve RNA integrity[52]. Overall, processing ocular tissues using the optimized protocol with alcohol-based staining reagents yielded consistent ocular-tissue sections that were fully immobilized on the PET membrane slide.

Our goal for this study was to develop a robust and reliable method for isolating high quality mRNA from the TM of mouse eyes for downstream expression analysis in order to obtain insights into the molecular mechanisms that underlie elevated IOP and glaucoma. As shown in the heatmap in **Figure 7C**, the described protocol of isolating TM by LCM provides a very reliable method to isolate RNA from TM and study differences in gene expression in TM from wild type and mutant mice. The method described herein will allow investigators to perform molecular analysis on a tissue central to the pathogenesis of glaucoma in an *in vivo* system that is relatively easy and reliable and can be applied to gene expression analysis.

Disclosures

The authors have nothing to disclose.

References

1. Foster, P. J., Buhrmann, R., Quigley, H. A., & Johnson, G. J. The definition and classification of glaucoma in prevalence surveys. *British Journal of Ophthalmology.* **86** (2), 238-242 (2002).
2. Quigley, H. A. Glaucoma. *Lancet.* **377** (9774), 1367-1377 (2011).
3. Dismuke, W. M., Overby, D. R., Civan, M. M., & Stamer, W. D. The Value of Mouse Models for Glaucoma Drug Discovery. *Journal of Ocular Pharmacology and Therapeutics.* **32** (8), 486-487 (2016).
4. Quigley, H. A. Number of people with glaucoma worldwide. *British Journal of Ophthalmology.* **80** (5), 389-393 (1996).
5. Quigley, H. A., & Broman, A. T. The number of people with glaucoma worldwide in 2010 and 2020. *British Journal of Ophthalmology.* **90** (3), 262-267 (2006).
6. Resnikoff, S. *et al.* Global data on visual impairment in the year 2002. *Bulletin World Health Organization.* **82** (11), 844-851 (2004).
7. Thylefors, B., Negrel, A. D., Pararajasegaram, R., & Dadzie, K. Y. Global data on blindness. *Bulletin World Health Organization.* **73** (1), 115-121 (1995).
8. Comparison of glaucomatous progression between untreated patients with normal-tension glaucoma and patients with therapeutically reduced intraocular pressures. Collaborative Normal-Tension Glaucoma Study Group. *American Journal of Ophthalmology.* **126** (4), 487-497 (1998).
9. The effectiveness of intraocular pressure reduction in the treatment of normal-tension glaucoma. Collaborative Normal-Tension Glaucoma Study Group. *American Journal of Ophthalmology.* **126** (4), 498-505 (1998).
10. The Advanced Glaucoma Intervention Study (AGIS): 7. The relationship between control of intraocular pressure and visual field deterioration. The AGIS Investigators. *American Journal of Ophthalmology.* **130** (4), 429-440 (2000).
11. Anderson, D. R. Collaborative normal tension glaucoma study. *Current Opinion Ophthalmology.* **14** (2), 86-90, (2003).
12. Kass, M. A. *et al.* The Ocular Hypertension Treatment Study: a randomized trial determines that topical ocular hypotensive medication delays or prevents the onset of primary open-angle glaucoma. *Archives of Ophthalmology.* **120** (6), 701-713, (2002).
13. Gordon, M. O. *et al.* The Ocular Hypertension Treatment Study: baseline factors that predict the onset of primary open-angle glaucoma. *Archives of Ophthalmology.* **120** (6), 829-730, (2002).
14. Leske, M. C. *et al.* Factors for glaucoma progression and the effect of treatment: the early manifest glaucoma trial. *Archives of Ophthalmology.* **121** (1), 48-56, (2003).
15. Chen, S., & Zhang, X. The Rodent Model of Glaucoma and Its Implications. *Asia-Pacific Journal Ophthalmology (Phila).* **4** (4), 236-241 (2015).
16. Fernandes, K. A. *et al.* Using genetic mouse models to gain insight into glaucoma: Past results and future possibilities. *Experimental Eye Research.* **141**, 42-56 (2015).
17. Howell, G. R., Libby, R. T., & John, S. W. Mouse genetic models: an ideal system for understanding glaucomatous neurodegeneration and neuroprotection. *Progress in Brain Research.* **173** 303-321 (2008).
18. John, S. W., Anderson, M. G., & Smith, R. S. Mouse genetics: a tool to help unlock the mechanisms of glaucoma. *Journal of Glaucoma.* **8** (6), 400-412, (1999).
19. Braunger, B. M., Fuchshofer, R., & Tamm, E. R. The aqueous humor outflow pathways in glaucoma: A unifying concept of disease mechanisms and causative treatment. *Eurupean Journal of Pharmaceutics and Biopharmaceutics.* **95** (Pt B), 173-181 (2015).
20. Weinreb, R. N. *et al.* Primary open-angle glaucoma. *Nature Reviews Disease Primers.* **2** (16067) (2016).
21. Burdon, K. P. Genome-wide association studies in the hunt for genes causing primary open-angle glaucoma: a review. *Clinical and Experimental Ophthalmology.* **40** (4), 358-363 (2012).
22. Iglesias, A. I. *et al.* Genes, pathways, and animal models in primary open-angle glaucoma. *Eye (London).* **29** (10), 1285-1298 (2015).
23. Jakobs, T. C. Differential gene expression in glaucoma. *Cold Spring Harbor Perspectives in Medicine.* **4** (7) (2014).

24. Jeck, W. R., Siebold, A. P., & Sharpless, N. E. Review: a meta-analysis of GWAS and age-associated diseases. *Aging Cell.* **11** (5), 727-731 (2012).
25. Sakurada, Y., & Mabuchi, F. Advances in glaucoma genetics. *Progress in Brain Research.* **220**, 107-126 (2015).
26. Agarwal, R., & Agarwal, P. Rodent models of glaucoma and their applicability for drug discovery. *Expert Opinion on Drug Discovery.* **12** (3),1-10 (2017).
27. Aires, I. D., Ambrosio, A. F., & Santiago, A. R. Modeling Human Glaucoma: Lessons from the in vitro Models. *Ophthalmic Research.* **57** (2), 77-86 (2016).
28. Burgoyne, C. F. The non-human primate experimental glaucoma model. *Experimental Eye Research.* **141**, 57-73 (2015).
29. Morgan, J. E., & Tribble, J. R. Microbead models in glaucoma. *Experimental Eye Research.* **141**, 9-14 (2015).
30. Morrison, J. C., Cepurna, W. O., & Johnson, E. C. Modeling glaucoma in rats by sclerosing aqueous outflow pathways to elevate intraocular pressure. *Experimental Eye Research.* **141**, 23-32 (2015).
31. Overby, D. R., & Clark, A. F. Animal models of glucocorticoid-induced glaucoma. *Experimental Eye Research.* 141, 15-22 (2015).
32. Rybkin, I., Gerometta, R., Fridman, G., Candia, O., & Danias, J. Model systems for the study of steroid-induced IOP elevation. *Experimental Eye Research.* **158**, 51-58 (2016).
33. Zernii, E. Y. *et al.* Rabbit Models of Ocular Diseases: New Relevance for Classical Approaches. *CNS & Neurological Disorders - Drug Targets.* **15** (3), 267-291 (2016).
34. Gong, H., Ruberti, J., Overby, D., Johnson, M., & Freddo, T. F. A new view of the human trabecular meshwork using quick-freeze, deep-etch electron microscopy. *Experimental Eye Research.* **75** (3), 347-358 (2002).
35. Hoerauf, H. *et al.* Transscleral optical coherence tomography: a new imaging method for the anterior segment of the eye. *Archives of Ophthalmology.* **120** (6), 816-819 (2002).
36. Tomarev, S. I., Wistow, G., Raymond, V., Dubois, S., & Malyukova, I. Gene expression profile of the human trabecular meshwork: NEIBank sequence tag analysis. *Investigative Ophthalmology & Visual Science.* **44** (6), 2588-2596, (2003).
37. Kim, B. S. *et al.* Targeted disruption of the myocilin gene (Myoc) suggests that human glaucoma-causing mutations are gain of function. *Molecular and Cellular Biology.* **21** (22), 7707-7713 (2001).
38. Gould, D. B. *et al.* Genetically increasing Myoc expression supports a necessary pathologic role of abnormal proteins in glaucoma. *Molecular and Cellular Biology.* **24** (20), 9019-9025 (2004).
39. Teixeira, L., Zhao, Y., Dubielzig, R., Sorenson, C., & Sheibani, N. Ultrastructural abnormalities of the trabecular meshwork extracellular matrix in Cyp1b1-deficient mice. *Veterinary pathology.* **52** (2), 397-403 (2015).
40. Hackler, L., Masuda, T., Oliver, V. F., Merbs, S. L., & Zack, D. J. Use of laser capture microdissection for analysis of retinal mRNA/miRNA expression and DNA methylation. *Retinal Development: Methods and Protocols.* **884**, 289-304 (2012).
41. Gipson, I. K., Spurr-Michaud, S., & Tisdale, A. Human conjunctival goblet cells express the membrane associated mucin MUC16: Localization to mucin granules. *Experimental Eye Research.* **145**, 230-234 (2016).
42. Sweigard, J. H. *et al.* The alternative complement pathway regulates pathological angiogenesis in the retina. *The FASEB Journal.* **28** (7), 3171-3182 (2014).
43. Marko, C. K. *et al.* Spdef null mice lack conjunctival goblet cells and provide a model of dry eye. *The American Journal of Pathology.* **183** (1), 35-48 (2013).
44. Huynh, S., & Otteson, D. Optimizing Laser Capture Microdissection to Study Spatiotemporal Gene Expression in the Retinal Ganglion Cell Layer. *Investigative Ophthalmology & Visual Science.* **54** (15), 2469-2469, (2013).
45. Cone, F. E., Gelman, S. E., Son, J. L., Pease, M. E., & Quigley, H. A. Differential susceptibility to experimental glaucoma among 3 mouse strains using bead and viscoelastic injection. *Experimental Eye Research.* **91** (3), 415-424 (2010).
46. McKinnon, S. J., Schlamp, C. L., & Nickells, R. W. Mouse models of retinal ganglion cell death and glaucoma. *Experimental Eye Research.* **88** (4), 816-824 (2009).
47. Schroeder, A. *et al.* The RIN: an RNA integrity number for assigning integrity values to RNA measurements. *BMC Molecular Biology.* **7** (3) (2006).
48. Hardy, K. M., Hoffman, E. A., Gonzalez, P., McKay, B. S., & Stamer, W. D. Extracellular trafficking of myocilin in human trabecular meshwork cells. *Journal of Biological Chemistry.* **280** (32), 28917-28926 (2005).
49. Morgan, J. T. *et al.* Human trabecular meshwork cells exhibit several characteristics of, but are distinct from, adipose-derived mesenchymal stem cells. *Journal of Ocular Pharmacology and Therapeutics.* **30** (2-3), 254-266 (2014).
50. Hindson, C. M. *et al.* Absolute quantification by droplet digital PCR versus analog real-time PCR. *Nature Methods.* **10** (10), 1003-1005 (2013).
51. Wang, W. Z., Oeschger, F. M., Lee, S., & Molnar, Z. High quality RNA from multiple brain regions simultaneously acquired by laser capture microdissection. *BMC Molecular Biology.* **10** (69) (2009).
52. Cummings, M. *et al.* A robust RNA integrity-preserving staining protocol for laser capture microdissection of endometrial cancer tissue. *Analytical Biochemistry.* **416** (1), 123-125 (2011).

